Drug Design, Development and Therapy

Dovepress
open access to scientific and medical research

Open Access Full Text Article

ORIGINAL RESEARCH

Dexmedetomidine Ameliorates Cardiac Ischemia/Reperfusion Injury by Enhancing Autophagy Through Activation of the AMPK/SIRT3 Pathway

Hong He[1], Peng Liu[2], Peng Li[1]

[1]Department of Anesthesiology, Sichuan Provincial People's Hospital, School of Medicine, University of Electronic Science and Technology of China, Chengdu, Sichuan, 610072 People's Republic of China; [2]Department of Anesthesiology, West China Second University Hospital, Sichuan University, Chengdu, Sichuan, 610044 People's Republic of China

Correspondence: Peng Li, Department of Anesthesiology, Sichuan Provincial People's Hospital, School of Medicine,University of Electronic Science and Technology of China, No. 32, West Section 2, 1st Ring Road, Chengdu, Sichuan, 610072, People's Republic of China, Tel +86 13668169590, Email lipengmazui@163.com

Objective: Myocardial ischemia-reperfusion (I/R) injury is a detrimental disease, resulting in high morbidity and mortality globally. In this study, we aimed to investigate the role of Dex in mitigating cardiac I/R injury.

Methods: H9c2 cells were treated with Dex (1 μM) for 24 h followed by oxygen-glucose deprivation/re-oxygenation (OGD/R). *ANP* and *BNP* mRNA of H9c2 cells and the LDH release were measured. Apoptosis of H9c2 cells was analyzed by flow cytometry. Mitochondrial membrane potential and superoxide production were detected by JC-1 staining and MitoSOX^{TM} Red, respectively. Cell aerobic respiration was measured using Seahorse analysis. In vivo, mice were injected with Dex (25 μg/kg, i.p., once daily) for 5 days and then subjected to heart I/R. Heart function was analyzed by echocardiography. CK-MB and LDH were measured by Elisa. Infarct size was measured using TTC-Evans blue staining. Mitochondrial ultrastructure was observed using transmission electron microscopy. DHE staining, SOD activity, the content of MDA, and the content of GSH/GSSG of heart were measured to evaluate the oxidative stress. In addition, inflammatory cytokines were measured in vivo and in vitro. Furthermore, AMPK, SIRT3, and autophagy-related protein expression in the heart were detected by Western blot.

Results: Dex reduced the H9c2 cells injury exposed to OGD/R, accompanied by improved mitochondrial function and membrane potential. In vivo, Dex improved heart function, myocardial injury, and the mitochondria ultrastructure following I/R injury. Meanwhile, Dex inhibited myocardial oxidative stress and inflammation in the myocardial I/R. Furthermore, Compound C (an AMPK inhibitor) could inhibit Dex-induced autophagy in the I/R heart and the 3-MA (an autophagy inhibitor) could partially interfere with the effects of Dex on the protection of I/R heart.

Conclusion: Dex suppressed oxidative stress and inflammation by promoting autophagy through activating the AMPK/SIRT3 pathway, thus protecting the heart against the I/R injury.

Keywords: dexmedetomidine, cardiac ischemia reperfusion, autophagy, AMPK/SIRT3

Introduction

Acute myocardial infarction is a leading cause of mortality worldwide, and reperfusion is the primary strategy for inhibiting myocardial infarction.[1,2] However, the process of reperfusion paradoxically triggers a cascade of necrotic and apoptotic cell death processes that progressively undermine cardiac contractility, thus giving rise to myocardial ischemia/reperfusion (I/R) injury.[3,4] Aberrant ROS production and mitochondrial dysfunction have emerged as pivotal mechanisms underlying the pathophysiology of cardiac I/R injury.[3,5,6] During I/R, excessive production of ROS primarily originates from mitochondria, leading to mitochondrial dysfunction, ATP depletion, and subsequent cardiac impairment.[6–8] Therefore, there is an urgent need to explore novel therapeutic strategies capable of effectively inhibiting oxidative stress and maintaining a dynamic equilibrium in mitochondria, which is crucial for preventing early pathological changes during I/R and enhancing the heart's resistance to I/R injury.

Received: 2 August 2023
Accepted: 13 October 2023
Published: 25 October 2023

Dex, a highly selective and potent α2 adrenergic agonist, is widely used in clinical anesthesia and the intensive care unit for sedation and analgesia with minimal suppression of respiratory function.[9] Accumulating evidence has demonstrated that Dex confers anti-inflammatory and antioxidant properties to attenuate brain injury induced by I/R[10] and lipopolysaccharide in animal models.[11,12] Additionally, Dex was reported to possess cytoprotective effects against acute kidney injury and lung injury by mitigating oxidative stress and mitochondrial damage.[13–15] Clinical studies also confirmed that Dex could induce a low incidence and severity of adverse safety events in infants receiving cardiopulmonary bypass, usually undergoing cardiac I/R injury. Although studies have reported the protective effects of Dex on myocardial I/R injury, the mechanism is not clear.[16–18]

Autophagy, an evolutionarily conserved degradation process, helps to remove damaged proteins and organelles.[19] The process of autophagy in the heart is constitutively active and further modulated under stress conditions such as starvation, ischemia, and hypoxia.[20,21] However, a contentious debate persists regarding the protective or detrimental role of autophagy in myocardial I/R injury.[22–24] Previous studies have demonstrated that autophagy flux is increased following the generation of large amounts of ROS in the myocardium during I/R. Excessive ROS induces the blocking of autophagic flux while resulting in the accumulation of microtubule-associated proteins 1 light chain 3 (LC3) II and p62 (an autophagy-specific target protein).[7,22] Physiologically, dysfunctional mitochondria are rapidly cleared by autophagy processes, and functional autophagy along with mitophagy is critical for maintaining mitochondrial quality to protect against myocardial I/R injury.[23–25]

Nowadays, SIRT3-induced autophagy has been implicated in the pathogenesis of myocardial I/R injury. SIRT3 interacts with various proteins, including AMP-activated protein kinase (AMPK), and is especially sensitive to energy stress conditions such as I/R.[26,27] When cellular energy is insufficient, activation of AMPK restores the energy equilibrium by stimulating catabolic processes that generate ATP and suppressing assimilation processes that consume ATP.[26,28] Previous studies showed that both AMPK and SIRT3 have been activated under energy deprivation and ischemia.[28,29] Also, Dex has the ability to enhance AMPK/SIRT3 expression in Parkinson's disease and kidney injury.[30,31] Thus, we propose that Dex may augment autophagy and protect against cardiac I/R injury, potentially through the activation of the AMPK/SIRT3 pathway.

In this study, we employed in vitro and in vivo I/R models to validate the suppressive effects of Dex on myocardial oxidative stress and functional impairments, which ultimately improved myocardial I/R injury and prevented cardiac function deterioration. Mechanistically, Dex promoted the AMPK/SIRT3 pathway and enhanced autophagy for cardiac energy homeostasis. Our research might present a new therapy for ischemic heart disease and expand the application prospects of Dex in cardiopulmonary bypass surgery.

Materials and Methods

Reagents

Dexmedetomidine (#PHR2118) was purchased from Jiangsu Hengrui Pharmaceuticals Co., Ltd. (China). Compound C (#S7306) and 3-Methyladenine (3-MA, #S1075) were purchased from Selleck (Shanghai, China). 4′,6-diamidino-2-phenylindole (DAPI) and JC-1 (#T4069) were purchased from Sigma-Aldrich, Inc. (St. Louis, US). MitoSOX^{TM} Red (#M36007) was purchased from Thermo Fisher (Waltham, MA, US). Malondialdehyde (MDA, #S0131S), Superoxide dismutase (SOD, #S0101S), Glutathione (GSH, #S0053), ATP content (#S0026), and NAD^+/NADH (#S0175) assay kits were purchased from Beyotime Biotechnology (Shanghai, China). Elisa kits of interleukin 1 beta (IL-1β, #E-EL-R0012c), interleukin-6 receptor (IL-6, #E-EL-R0015c), and tumor necrosis factor-alpha (TNF-α, #EMSEL-R2856c) were purchased from Elabscience Biotechnology Co., Ltd. (Wuhan, Hubei, China). Elisa kits of creatine kinase (CK-MB, #8671) and lactate dehydrogenase (LDH, #12239) were purchased from Meimian Industrial Co., Ltd. (Nanjing, Jiangsu, China). Primary antibodies against AMPK alpha 1 (#ab32047), LC3B (#ab192890) and p62 (#ab109012), and secondary antibodies (#ab6789) were purchased from Abcam Inc. (Boston, MA, USA). Primary antibodies against SIRT3 (#10099-1-AP), PINK1 (#23274-1-AP), Parkin (#14060-1-AP), and GAPDH (#60004-1-AP) were purchased from Proteintech Inc. (Wuhan, Hubei, China).

Animals and Treatment

This study was performed following the approval of the Ethics Committee of Sichuan Provincial People's Hospital (#2022-161) in accordance with the Guide for the Care and Use of Laboratory Animals provided by the National Institutes of Health

(NIH). Male 7–8-week-old C57BL/6 mice (23 ± 2 g) were purchased from Gempharmatech Co., Ltd. (Nanjing, Jiangsu, China) and housed under specific pathogen-free conditions (12 h light/dark cycles and 24 ± 2°C) with free access to food and water. According to previous studies,[15,31] mice in the I/R+Dex group were injected with Dex (25 μg/kg, i.p.) once a day for 5 days, followed by the I/R process. Mice in the control group and I/R group were intraperitoneally injected with an equal volume of saline. Mice in the I/R+Dex+Compound C group received intraperitoneal injections of Dex for 5 days and were subjected to Compound C (10 mg/kg; i.p.) before the I/R operation. Additionally, mice in the I/R+Dex+3-MA group received the same treatment for 5 days and were subjected to 3-MA (20 mg/kg; i.p.) before the surgery. There were 6 mice per group, and all efforts were made to reduce the consumption of mice.

To generate the heart I/R injury, the left anterior descending coronary artery (LAD) was ligated for 30 min and repercussed for 24 h, as previously described.[7,29] In brief, mice were anesthetized by intraperitoneal injection of ketamine (120 mg/kg) and xylazine (4 mg/kg), intubated, and ventilated with pure O_2 using a MiniVent mouse ventilator (Model 845, Harvard Apparatus). Body temperature was kept at a warm surgical platform. After the heart was exposed by a left thoracotomy, the LAD artery 1mm below the tip of the left atrial appendage was ligated with a 7–0 silk suture (US Surgical Corp., Norwalk, Connecticut) over a piece of PE-10 tubing for 30 minutes. Ischemia was confirmed by both ST elevation on the surface electrocardiogram and visual blanching. Reperfusion was accomplished by releasing the ligature, and the chest was closed in layers.

Next, cardiac function was evaluated at baseline and after 24 h of reperfusion using the Vevo 2100 Imaging (Visual Sonics, Toronto, Canada) echocardiographic system equipped with a 30 MHz transducer. The mice were anesthetized with isoflurane in O_2 gas. After anesthetization, each mouse was placed on a heated imaging platform. The following parameters —left ventricular ejection fraction (LVEF%) and left ventricular fractional shortening (LVFS%) were calculated.

Cells

H9c2 rat myocardial cells obtained from the American Type Culture Collection (ATCC; Rockville, MD, USA) were cultured in high-glucose DMEM supplemented with 10% (v/v) FBS, 100 U/mL penicillin, and 100 mg/mL streptomycin at 37°C in humidified air containing 5% CO_2. To determine the effects of Dex, the H9c2 cells were treated with 1 μM Dex for 24 h, according to a previous study.[32]

Cell Viability Assay

H9c2 cells were exposed to the indicated concentrations of Dex (1 nM; 10 nM; 1 μM; 5 μM) for 24 h, and the cell's viability was assessed using the CCK-8 (Dojindo Molecular Technologies, Kyushu, Japan).[33] Cells were mixed with the CCK-8 reagent for 1 hour at 37°C in humidified air containing 5% CO_2. The absorbance under 450 nm was detected using a microplate reader (Bio-Rad, Hercules, CA). Cell viability was calculated as the percentage of absorbance compared with control cells.

Oxygen Glucose Deprivation/Reperfusion (OGD/R)

H9c2 cells were rinsed twice with glucose-free DMEM, and the culture medium was replaced with glucose-free DMEM supplemented with 10% FBS and 1% penicillin/streptomycin (pre-balanced in an O_2-free chamber at 37°C). Then, cells were immediately placed in a sealed chamber loaded with mixed gas containing 5% CO_2 and 95% N_2 at 37°C for 6 h. Afterwards, cells were refreshed with the normal medium and cultured at 37°C for 24 h in humidified air containing 5% CO_2 for reperfusion.

LDH Release

LDH assay kits (#ab65393) were purchased from Abcam Inc. (Boston, MA, USA) and used to determine the LDH release in the supernatant of cell culture medium according to the manufacturer's instructions. The colorimetric change of cells at 492 nm was obtained with a microplate reader.

Cell Apoptosis

Apoptosis of H9c2 cells was detected using the Annexin V-PI staining assay kit (Beyotime, #C1062) and analyzed using flow cytometry (Beckman Coulter cytoFLEX, USA). Briefly, cells that stained positive for Annexin-V were counted as apoptotic cells (Annexin VFITC, Ex/Em: 488 nm/525 nm; PI, Ex/Em: 561 nm/575 nm). The total cell number was counted using DAPI staining, and the average staining-positive cell ratio was calculated. The apoptosis rate means early apoptosis (Q2 of the flow cytometry dot plot) and late apoptosis (Q3 of the flow cytometry dot plot).

Mitochondrial Membrane Potential

The mitochondrial membrane potential was determined by JC-1 staining. H9c2 cells were incubated with JC-1 (2 μM) for 20 min at 37°C, washed with culture medium, and visualized using fluorescence microscopy (DMI 3000B, Leica, Wetzlar, Germany). The fluorescence intensity changes were analyzed using a microplate reader. For JC-1 monomers (green), the excitation and emission wavelengths of JC-1 were set at 490 nm and 530 nm, respectively. For JC-1 aggregates (red), the corresponding values were 525 nm and 590 nm. Fluorescence intensity was measured using Image J (NIH).

Mitochondrial Superoxide Production

H9c2 cells were incubated with MitoSOX^{TM} Red (3 μM) at 37°C for 30 min, followed by washing twice and being resuspended in PBS for flow cytometry analysis (Ex/Em: 510 nm/580 nm). Fluorescence intensity was measured using Image J.

Mitochondrial Oxygen Consumption Rate (OCR)

H9c2 cells aerobic respiration was measured with a Seahorse XF24 analyzer (Agilent Technologies, Santa Clara, CA) as described previously.[22,34] Briefly, cells were planted overnight on 24-well polystyrene Seahorse plates. H9c2 cells were washed and cultured with Seahorse assay mediums containing 2 mM glutamine, 1 mM pyruvate, and 10 mM glucose in a non-CO_2 incubator at 37°C for 1 h before the assay. The baseline measurements were obtained first, followed by the sequential injection of oligomycin A (5 μM final concentration, MCE), FCCP (3 μM final concentration, MCE), and Rotone/Antimycin A (1 μM/l μM final concentration, Sigma) at 37°C. The respiratory rates are reported as oxygen flux per mass, and all readings are normalized to cell number (pmolO_2/min 10,000 cells).

Tetrazolium Chloride (TTC)-Evans Blue Staining

I/R-induced myocardial infarction was determined by TTC-Evans blue staining as described previously.[7,22] Briefly, after 24 hours of reperfusion, the heart was quickly excised. After washing out the blood with saline, 0.2 mL of 1% Evans blue dye was injected through the aortic root. The hearts were sliced transversally into 1-mm-thick sections and 5–6 sections per heart, starting from the apex. The sections were immersed in 1% TTC (dissolved in PBS) at 37°C for 15 min and then fixed in a 4% paraformaldehyde solution for 24 h at room temperature. The area at risk (AAR) was identified by the absence of blue dye. The total LV area, AAR, and TTC-negative staining area (infarcted myocardium) were measured with Image J.

Enzyme-linked Immunosorbent Assay (Elisa)

Elisa kits for IL-1β, IL-6, and TNF-α were employed to detect the levels of inflammatory cytokines in the medium of H9c2 cells according to the supplier's instructions. Elisa kits for CK-MB and LDH were employed to detect the levels of cardiac injury markers in the plasma of mice according to the supplier's instructions.

Dihydroethidine (DHE) Staining

Cardiac tissues were embedded in the Tissue-Tek OCT compound (Sakura Finetek, Tokyo, Japan) and serially sectioned to 10-μm thickness. The cryosections were stained with the superoxide-sensitive dye DHE (10 μM in 0.01% DMSO) and incubated for 30 min at 37°C in a humidified dark chamber. All sections were photographed under an inverted fluorescence microscope (IX83, Olympus, Japan).

Evaluation of Oxidative Stress Status in vivo

The SOD activity, the MDA levels, and the GSH/GSSG content in the heart tissue were detected by using commercially available assay kits according to the manufacturer's instructions.

Transmission Electron Microscopy

The cardiac tissues were fixed for 24 h in 3% glutaraldehyde and then fixed with 1% osmium tetroxide for 1 h. Then, the samples were dehydrated in a series of ethanol, stained en bloc with 2% uranyl acetate, and embedded in Embed 812 for evaluation by electron microscopy (JEM-1400PLUS, JEOL, Japan). The images were assessed in a blinded fashion by pathologists.

ATP Content

Intracellular ATP levels were examined using an ATP content assay kit according to the manufacturer's protocol. Briefly, heart tissues were lysed in ATP lysis buffer. After centrifugation at 13,000 g for 15 min at 4°C, the supernatant was detected at an absorbance of 560 nm. The calculated content of ATP was normalized against the wet tissue weight using ATP standards and expressed as nmol/g tissue.

NAD^+/NADH Levels

Intracellular NAD^+/NADH in heart tissues was examined using the NAD^+/NADH assay kit with WST-8 according to the manufacturer's protocol.

Quantitative Polymerase Chain Reaction (qPCR)

RNA was extracted from the H9c2 cells or heart tissues using the TRIzol method. cDNA was synthesized from RNA using the FastKing One-Step RT-PCR Kit from Tiangen Biotech Co., Ltd. (Beijing, China). All primers were purchased from TSINGKE Biosystems (Beijing, China). Quantitative real-time PCR was performed with SYBR Green from Bio-Rad (Hercules, CA, USA). Gene expression was calculated by the $2^{\Delta\Delta Ct}$ method and normalized to GAPDH levels.

The sequences of rat primers used are below:

ANP: F,5′-CTGGACTGGGGAAGTCAACC-3′; R,5′- CAATCCTACCCCCGAAGCAG-3′;

BNP: F,5′-GCTGCTGGAGCTGATAAGAGAA-3′; R,5′- GCGCCAATCCGGTCTATCTT-3′;

GAPDH: F,5′-GAAGGTCGGTGTGAACGGAT-3′; R,5′- CCCATTTGATGTTAGCGGGAT-3′.

The sequences of mouse primers used are below:

IL-1β: F,5′-GCAACTGTTCCTGAACTCAACT-3′, R,5′- ATCTTTTGGGGTCCGTCAACT-3′;

IL-6: F,5′-CCAAGAGGTGAGTGCTTCCC-3′; R,5′- CTGTTGTTCAGACTCTCTCCCT-3′;

TNF-α: F,5′-GTCGTAGCAAACCACCAAGC-3′; R,5′-TGTGGGTGAGGAGCACATAG-3′;

GAPDH: F,5′-ATCTTTTGGGGTCCGTCAACT-3′; R,5′-TTTGCACTGGTACGTGTTGAT-3′.

Western Blot

Heart tissues were lysed with RIPA lysis buffer with a protease inhibitor cocktail and then centrifuged at 13,000g for 15 min at 4°C. Protein extracts were separated by SDS-PAGE and transferred to PVDF membranes. The membrane was blocked in 5% non-fat milk and incubated with primary antibodies at 4°C overnight, including anti-AMPK, anti-SIRT3, anti-p62, anti-LC3, anti-Parkin, anti-PINK1, and anti-α-tubulin antibodies. After incubation with HRP-conjugated secondary antibodies, the signal intensities were visualized by an ECL Western blot detection kit (#P10100, ECM) and quantified by Image J.

Statistical Analysis

GraphPad Prism v.8.4 (GraphPad, La Jolla, CA) was employed for statistical analysis. The Shapiro–Wilk normality test was performed to determine the data distribution. All data were normally distributed and presented as the mean ± standard deviation (SD). Paired or unpaired, two-tailed Student's *t*-tests were selected to compare two groups. A one-way

analysis of variance (ANOVA), followed by Tukey's multiple comparisons test, was performed to determine the differences among > two groups. P values <0.05 were statistically significant.

Results

Dexmedetomidine Protects H9c2 Cells from OGD/R Injury

We treated H9c2 cardiomyocytes with Dex at several concentrations (1 nM; 10 nM; 1 μM; 5 μM) for 24 hours and did not observe cellular toxicity, which is consistent with the previous study[33] (Figure 1A). Therefore, we opted for a 1 μM Dex pretreatment in H9c2 cells prior to OGD/R. Remarkably, we found that OGD/R significantly increased the mRNA levels of *ANP* and *BNP* compared to the control group (Figure 1B). However, Dex treatment inhibited the expression of *ANP* and *BNP*, indicating that Dex attenuated cardiomyocyte injury induced by OGD/R (Figure 1B). The Annexin V-PI staining also revealed a significant increase in early apoptotic cells within the OGD/R-treated group compared to the control group. However, 1 μM Dex pretreatment for 24 hours effectively mitigated OGD/R-induced early apoptosis (Figure 1C–D). As a biomarker of cell death, LDH leakage surged in the OGD/R group in contrast with the control cells, while Dex reduced the LDH leakage remarkably (Figure 1E).

Ischemia/reperfusion injury often leads to mitochondrial damage in cardiomyocytes. The mitochondrial membrane potential (Ψm) of H9c2 cells exhibited a significant decrease in the ratio of red/green fluorescence intensity, while Dex treatment partially restored the mitochondrial membrane potential as reflected by the increased ratio of red/green fluorescence intensity (Figure 1F and G). We also observed that OGD/R harmed cellular aerobic respiration using Seahorse analysis, while Dex could alleviate the impaired cellular respiration, including the basal OCR and maximal

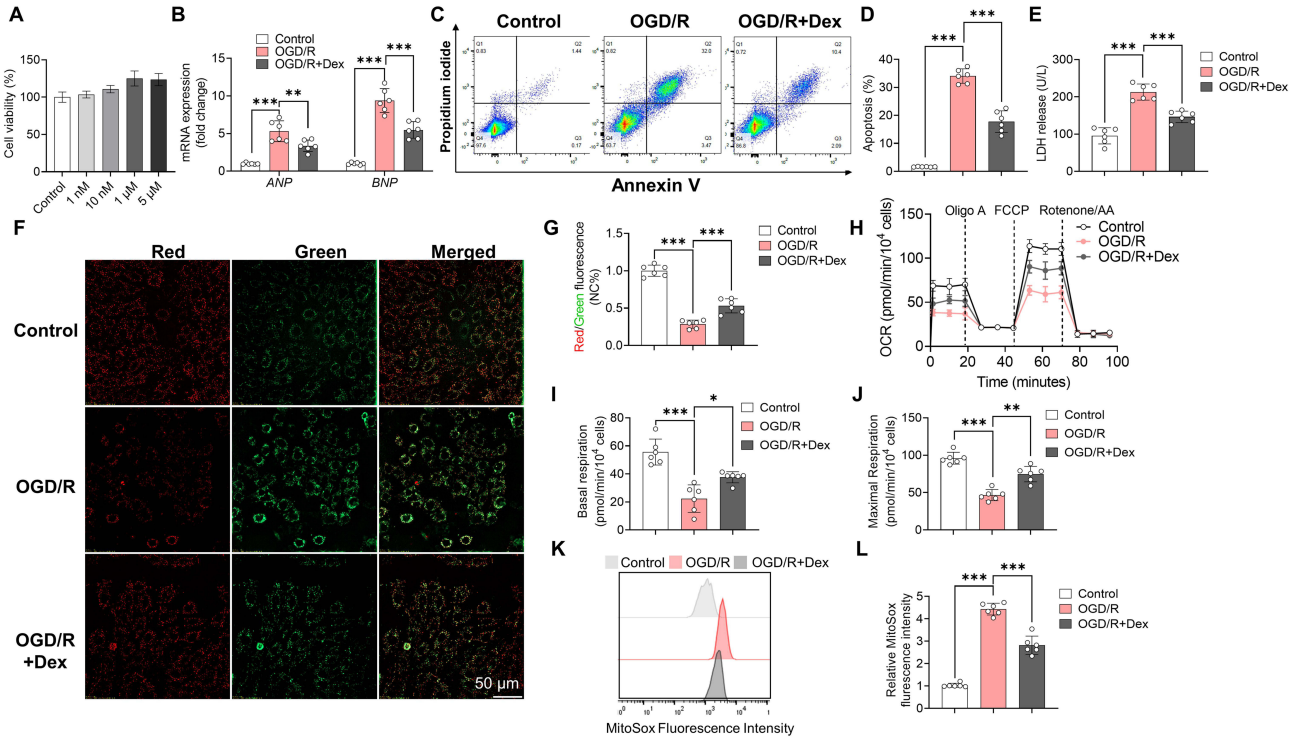

Figure 1 Dex alleviated OGD/R-induced apoptosis, membrane potential reduction, mitochondrial superoxide production, and improved aerobic respiration in H9c2 cells. (**A**). Detection the proliferation of H9c2 cells stimulated by different concentrations of Dex using the CCK-8 assay. (**B**). *ANP* and *BNP* mRNA expression in H9c2 cells. (**C**). Flow cytometry analysis for H9c2 cell apoptosis after Annexin V/PI staining. (**D**). Quantitative analysis of the apoptotic H9c2 cell. (**E**). LDH release in the medium of H9c2 cells. (**F**). Representative images of H9c2 cells stained with JC-1 for visualization of mitochondrial membrane potential. Aggregates were stained red, and monomers were stained green. 20 × magnification; Scale bar, 50 μm. (**G**). Analysis of the ratio of red/green fluorescent density relative to the control group. (**H–J**). Seahorse analysis for the cellular oxygen consumption rate (OCR) of H9c2 cells (**H**) and qualification of basal respiration (**I**) and maximum respiration (**J**). (**K** and **L**). Flow cytometry analysis (**K**) and quantification (**L**) of H9c2 cells stained with MitoSOX^{TM} Red for mitochondrial superoxide. Data are presented as the mean ± SD (n = 6) of at least three independent experiments. Statistical comparisons were conducted by one-way ANOVA, followed by Tukey's multiple comparisons test. *P < 0.05, **P < 0.01, and ***P < 0.001 for the indicated comparisons.

Abbreviation:NS, no significant difference.

OCR (Figure 1H–J). The mitochondria serve as the main generator of intracellular ROS under stress and are extremely susceptible to oxidative stress. ROS production within mitochondria was detected by the fluorescent superoxide indicator MitoSOX^{TM} Red (Figure 1K and L). Interestingly, Dex pretreatment for 24 h significantly suppressed the superoxide content induced by OGD/R (Figure 1K and L). These data collectively indicated that Dex inhibited oxidative stress and protected cardiomyocytes against OGD/R injury.

3.2 Dexmedetomidine improved heart function and attenuated cardiac injury following ischemia/reperfusion in vivo

To assess the impact of Dex on cardiac injury in vivo, we administered mice with Dex (25 μg/kg, i.p., once daily) for five days, followed by induction of cardiac I/R injury (Figure 2A). At baseline (before the I/R surgery), the heart function showed no difference, as reflected by the LVEF% and LVFS% (Figure 2B and C). Subsequently, I/R mice showed substantially reduced cardiac systolic function compared to the control group after 30 minutes of myocardial ischemia and 24 hours of reperfusion (Figure 2D–F). However, mice treated with Dex showed recovery in cardiac function to some extent, as reflected by the increased LVEF% and LVFS% in contrast with the I/R mice (Figure 2D–F). Furthermore, Dex-treated mice showed decreased levels of the cardiac injury biomarkers CK-MB and LDH in plasma (Figure 2G and H). Meanwhile, evaluation of myocardial infarct size was performed using TTC-Evans blue staining (Figure 2I–K). As is shown in Figure 2I, with the same risk area in both groups, the area of infarcted size (white) in the Dex-treated mice was much smaller than that in the I/R mice (Figure 2I–K). Moreover, we observed myocardial fiber rupture and disrupted mitochondrial ultrastructure, characterized by mitochondrial cristae disruption and loss, in the I/R heart using transmission electron microscopy (Figure 2L). Interestingly, treatment with Dex alleviated the abnormalities of mitochondrial ultrastructure induced by I/R and thus improved the ATP content in cardiomyocytes subjected to I/R (Figure 2M).

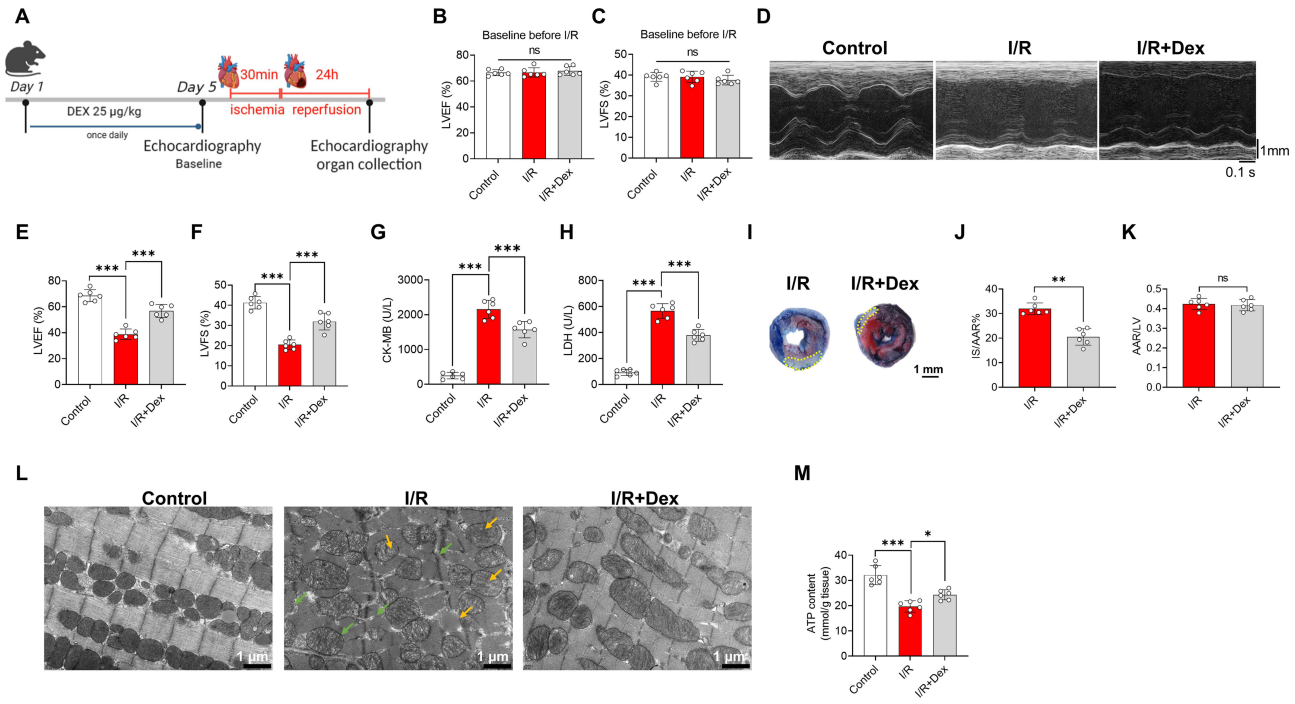

Figure 2 Dexmedetomidine protected mice against cardiac I/R injury and improved heart function following I/R. (**A**). Schematic flowchart of the application of Dex and the construction of the cardiac I/R model. (**B**–**C**). Left ventricular ejection fraction (LVEF%) and left ventricular fractional shortening (LVFS%) at baseline. (**D**). Representative images of M-mode echocardiography from mice. (**E** and **F**). LVEF% (**E**) and LVFS% (**F**) of mice. (**G** and **H**). Plasma CK-MB (**G**) and LDH (**H**) levels in mice. (**I**). Representative images of Evans-blue perfused and TTC-stained heart sections outlining the area at risk (AAR; sum of white and red areas); healthy viable tissue (blue); and infarcted tissue (pale white). Scale bar, 1 mm. (**J** and **K**). Quantification of infarct size relative to AAR (**J**) and AAR relative to LV (**K**). (**L**). Representative micrographs of the ventricular myocardium were observed by transmission electron microscopy. Fragmentation of muscle bands pointed by green arrows and abnormal shape of mitochondria, including swollen and absent cristae density pointed by Orange arrows. 6000 X magnification; Scale bar, 1 μm. (**M**). ATP content in heart tissues. Data are presented as the mean ± SD (n = 6). Statistical comparisons were conducted by an unpaired two-tailed Student's *t*-test or one-way ANOVA, followed by Tukey's multiple comparisons test. *P < 0.05, **P < 0.01, and ***P < 0.001 for the indicated comparisons.

Abbreviation:NS no significant difference.

Altogether, these results demonstrated that Dex can alleviate heart dysfunction and cardiac injury following ischemia/reperfusion in mice.

Dexmedetomidine Attenuated Myocardial Oxidative Stress and Inflammation Following Ischemia/Reperfusion

During ischemia/reperfusion injury, cardiomyocytes inevitably generate a large amount of ROS, accompanied by an exacerbated cascade of inflammation. Our in vitro experiments have confirmed the inhibitory effect of Dex on mitochondrial ROS after OGD/R. Subsequently, we investigated whether the benefits provided by Dex were conferred by suppressing oxidative stress. The fluorescence intensity of DHE-stained cardiac tissue in the border zone is increased in the I/R group, which suggests a high level of ROS production (Figure 3A). Moreover, increased levels of MDA, a product of lipid peroxidation, were observed in the hearts of I/R mice compared with the control mice (Figure 3B). In contrast, the activity of SOD (the major intracellular antioxidant) was inhibited after cardiac I/R injury (Figure 3C). Likewise, the levels of GSH were decreased and GSSG were increased in I/R hearts in contrast with the control mice (Figure 3D–F). However, the Dex-treated mice showed reduced fluorescence intensity of DHE, accompanied by lower MDA levels, enhanced SOD activity, and increased GSH levels, as well as an elevated ratio of GSH/GSSG compared to I/R mice (Figure 3A–F). Inflammation and oxidative stress are the main causes of mitochondrial dysfunction, contributing to impaired ATP production.[34–36] In light of the findings above, we conducted further investigation into the impact of Dex on cardiac inflammation in the context of I/R. Compared with the I/R mice, Dex suppressed the amplifying inflammation caused by I/R, as evidenced by the decreased mRNA levels of inflammatory cytokines including *IL-1β, IL-6*, and *TNF-α* within heart tissues (Figure 3G–I). The detection of inflammatory cytokine levels in the medium of H9c2 cells also favored that Dex inhibited the inflammatory response post-I/R (Figure 3J–L). These results suggested that Dex mitigated cardiac oxidative stress and inflammation, thus improving the heart's resistance to I/R injury in mice.

3.4. Dexmedetomidine enhanced autophagy through activation of the AMPK/SIRT3 pathway to attenuate cardiac I/R injury

The modulation of autophagy within myocardial cells has emerged as a novel strategy for myocardial protection.[25,37] Moderate autophagy eliminates cellular substances such as aggregated cytoplasmic proteins or damaged organelles, thereby reducing cell damage.[19,37] Hence, we aimed to investigate whether the protective effect of Dex on I/R injury is

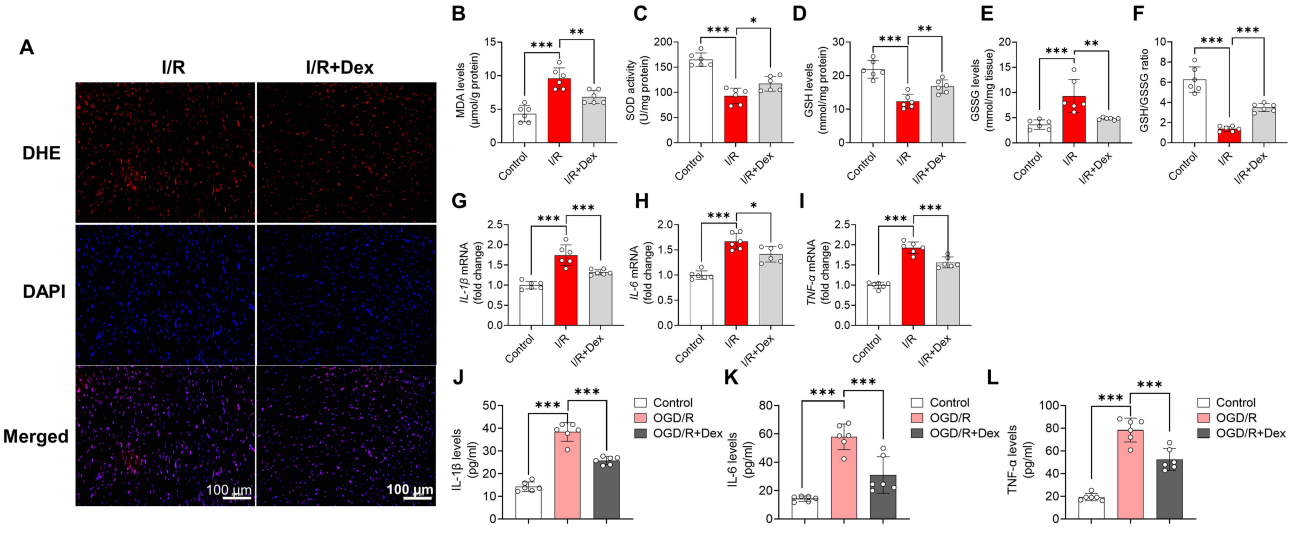

Figure 3 Dexmedetomidine attenuated oxidative stress and inflammation in the cardiac I/R. (**A**). Representative DHE staining of heart sections in the border zones. 20 X magnification; Scale bar, 100 μm. (**B**). MDA levels in heart tissues. (**C**). SDO activity in heart tissues. (**D–F**). GSH and GSSG content in heart tissues and the ratio of GSH/GSSG. (**G–I**). qPCR analysis for the mRNA levels of *IL-1β, IL-6*, and *TNF-α* in heart tissues. (**J–L**). Detection of IL-1β, IL-6, and TNF-α in the medium of H9c2 cells. Data are presented as the mean ± SD (n = 6) of at least three independent experiments. Statistical comparisons were conducted by one-way ANOVA, followed by Tukey's multiple comparisons test. *P < 0.05, **P < 0.01, and ***P < 0.001 for the indicated comparisons.
Abbreviation:NS, no significant difference.

mediated through autophagy, focusing on autophagy parameters including LC3 and p62. Compared to the control group, I/R mice exhibited increased protein levels of LC3 II and p62 within hearts, indicating blocked myocardial autophagic flux (Figure 4A–C). In contrast, the LC3 II and p62 levels showed the opposite trend in Dex-treated mice following I/R, indicating that Dex restores the blocked myocardial autophagic flux triggered by I/R (Figure 4A–C). Besides, the mitophagy-related proteins PINK1 and Parkin, which help to clear damaged mitochondria, are also increased by Dex after myocardial I/R injury, stressing the protective effect of Dex on mitochondrial homeostasis (Figure 4A and D).

Autophagy is crucial for cellular energy maintenance.[38] AMPK acts as an intracellular energy sensor under nutrition stress and hypoxia and subsequently activates downstream target SIRT3, which enhances autophagy to protect cells from mitochondrial dysfunction and oxidative stress.[28,38–40] Considering the potential beneficial effects of Dex on cardiac function and the autophagy process, we investigate the expression of AMPK and SIRT3 post-I/R injury. Our results revealed that the protein levels of AMPK and SIRT3 were decreased in hearts subjected to I/R (Figure 4A and D). However, treatment with Dex resulted in an upregulation of their expression in hearts post-I/R (Figure 4A and D). Noticeably, NAD^+, as the center of energy metabolism, is responsible for SIRT3 activity to maintain mitochondrial function and resistance to oxidative stress.[41,42] The administration of Dex significantly mitigated the I/R-induced reduction of the NAD^+/NADH ratio, thereby highlighting the role of Dex in preserving cardiac mitochondrial homeostasis during I/R. (Figure 4E). Furthermore, pre-treatment with Compound C to inhibit AMPK prior to I/R surgery resulted in a suppression of autophagy, as evidenced by the decreased expression levels of LC3 and p62 compared to the I/R+Dex group (Figure 4F–I), which is consistent with the effects observed upon administration of the autophagy inhibitor 3-MA (Figure 4J–L). Importantly, both Compound C and 3-MA partially attenuated the protective effect of Dex

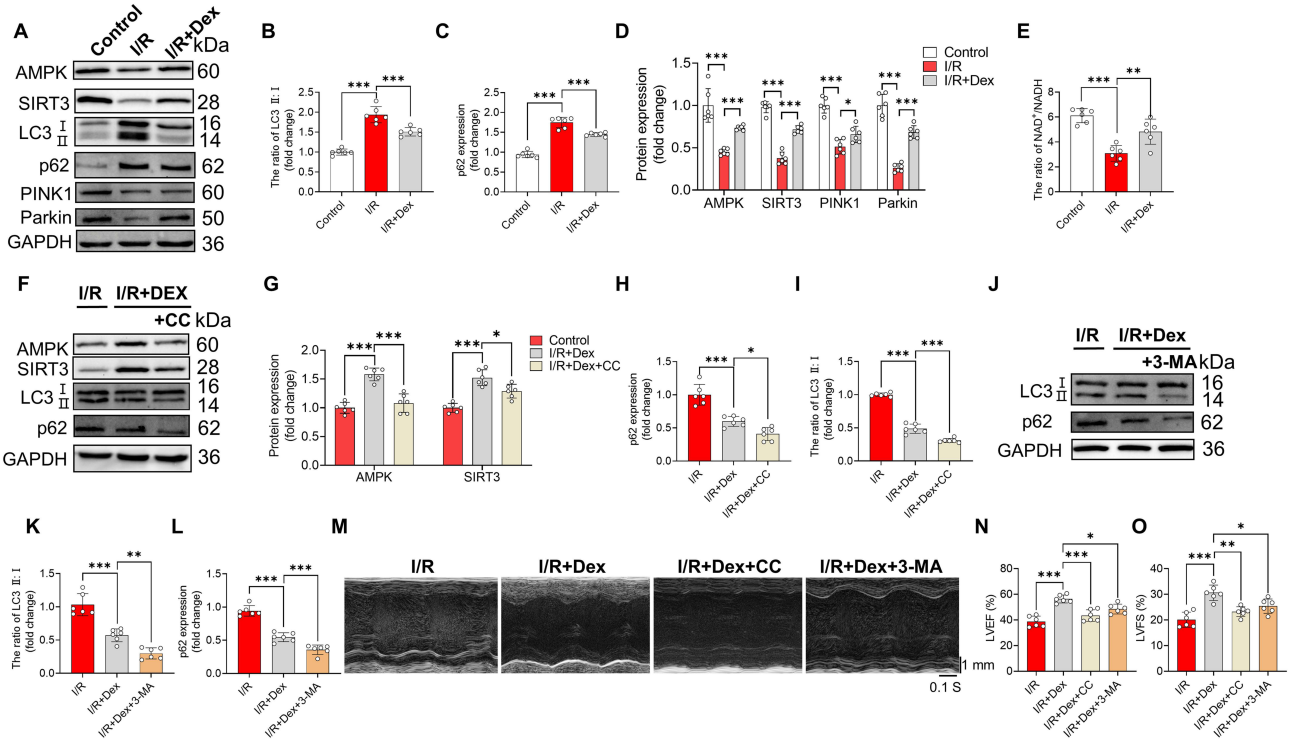

Figure 4 Dexmedetomidine enhanced autophagy for I/R heart protection through upregulation of the AMPK/SIRT3 pathway. (**A**). Representative images of immunoblots of hearts for the proteins LC3, p62, AMPK, SIRT3, PINK1, and Parkin. (**B** and **C**). Qualification of the ratio of LC3 II/I and p62 protein levels of hearts relative to the control mice. (**D**). Qualification of the AMPK, SIRT3, PINK1, and Parkin protein levels of hearts relative to the control mice. (**E**). The ratio of NAD^+/NADH in heart tissues. (**F–I**). Representative images of immunoblots of hearts for the proteins AMPK, SIRT3, LC3, and p62 and qualification for the expression relative to the I/R mice, including the additional Compound C-treated group. CC: Compound C. (**J–L**). Representative images of immunoblots of hearts for the proteins LC3 and p62 and qualification for the expression relative to the I/R mice, including the additional 3-MA-treated group. (**M**) Representative images of M-mode echocardiography from mice after indicated treatments post-I/R. (**N–O**). LVEF% (**N**) and LVFS% (**O**) from mice after indicated treatments post-I/R. =Data are presented as the mean ± SD (n = 6) and were performed in at least three independent experiments in vitro. Statistical comparisons were conducted by one-way ANOVA, followed by Tukey's multiple comparisons test. *P < 0.05, **P < 0.01, and ***P < 0.001 for the indicated comparisons.

Abbreviation: NS, no significant difference.

on the I/R heart, as evidenced by reduced cardiac function relative to Dex-treated mice (Figure 4M–O). These findings collectively indicated that Dex can protect against cardiac I/R injury by enhancing autophagy through activating the AMPK/SIRT3 pathway.

Discussion

Cardiac ischemia-reperfusion injury occurs when blood flow to the heart is temporarily interrupted and then restored.[1,3] While reperfusion is essential to salvage the ischemic tissue, it paradoxically exacerbates tissue damage.[2,6] The objective of this study was to investigate the therapeutic effects of Dex on cardiac I/R injury both in vivo and in vitro.

In this study, several concentrations of Dex were selected and showed no toxicity in cells. Next, we pretreated H9c2 cells with 1 μM Dex for 24 hours in accordance with a prior study to see how Dex affected myocardial cells exposed to OGD/R.[33] Consistent with previous studies, we found that Dex alleviated apoptosis and LDH release in OGD/R-treated H9c2 cells.[17,43] Overproduction of ROS, including superoxide anions, hydrogen peroxide, and hydroxyl radicals, contributed to oxidative stress and triggered a cascade of events leading to myocardial injury.[8,34,35] We found that OGD/R induced ROS bursts in H9c2 cells, while Dex inhibited superoxide production within mitochondria, as evidenced by reduced MitoSOX^{TM} red intensity. Mitochondria are not only the powerhouse of the cell but also a significant source of ROS.[8,35] Excessive ROS production degrades mitochondrial components, which can disrupt mitochondrial function and impair mitochondrial membrane potential.[5,6,8] The JC-1 labeling of H9c2 cells following OGD/R revealed that Dex had a positive impact on preserving mitochondrial membrane potential. Further Seahorse analysis confirmed that Dex may partially alleviate GOD/R-induced respiratory depression.

Afterwards, we initiated a mouse model of myocardial ischemia/reperfusion and evaluated the effects of Dex in vivo. We found that Dex significantly improved the declining cardiac function in I/R hearts, reduced the levels of cardiac injury markers CK-MB and LDH in plasma, and decreased the myocardial infarct size. In line with previous studies, disrupted mitochondrial integrity and depressed mitochondrial OXPHOS were observed in the I/R hearts.[27,34,44] Dex ameliorated the destruction of the mitochondrial ultrastructure and the myocardium and improved mitochondrial function, which restored ATP production in the I/R hearts. These findings highlight Dex's ability to prevent myocardial I/R injury in vivo, consistent with its function in vitro. Subsequently, we confirmed that Dex can significantly reduce ROS production in the I/R heart. MDA is a product of membrane lipid peroxidation, and Dex largely reduced the rise in MDA levels in cardiac tissue following I/R. Additionally, Dex also restored the vital antioxidant enzyme SOD activity in the I/R heart, along with increased GSH levels (another intracellular antioxidant). The accumulation of ROS activates inflammatory pathways and promotes the release of pro-inflammatory cytokines, exacerbating tissue damage and promoting cell death.[36,45] Several inflammatory factors can also be suppressed by Dex in I/R hearts and OGD/R-treated H9c2 cells, such as IL-1β, IL-6, and TNF-α. These findings compel us to investigate the potential mechanisms of Dex for cardiac protection post-I/R.

Recently, the interplay between ROS and autophagy has emerged as a significant avenue of research in understanding the pathophysiology of cardiac I/R injury.[21,25] Autophagy is responsible for degrading and recycling damaged organelles and proteins, which plays a crucial role in maintaining cellular homeostasis and mitigating various stress conditions.[21,38] However, the relationship between ROS and autophagy in cardiac I/R injury is complex and can have both protective and detrimental effects.[23,24,46] Moderate levels of ROS can stimulate autophagy as a protective mechanism against cellular stress.[46] Some studies utilizing in vitro and in vivo I/R models have suggested that inducing autophagy shows favorable effects against myocardial I/R injury.[4,47–49] Theoretically, autophagy is induced in response to stress, ie, damaged mitochondrial accumulation under hypoxia.[39,46] Conversely, excessive ROS can dysregulate autophagy, leading to impaired autophagic flux and the accumulation of dysfunctional autophagosomes, indicating that inhibiting autophagy exerts a protective effect against I/R injury.[25,50,51] Diverse observations in myocardial autophagy during the I/R process may be attributed to the differences in length of ischemia and reperfusion among different studies.[22,49,51] In this study, we emphasized the changes in myocardial autophagic flux after 24 hours of reperfusion. LC3 II is induced when autophagy initiates, and the specific protein p62 is degraded as autophagy progresses.[52] We observed that autophagy is impaired for 24 h of reperfusion, as manifested by the increase in LC3 II and p62 levels post-I/R, which suggested that autophagy is obstructed, thus failing to clear the damaged organelles post-I/R.[53] Interestingly, Dex helps to reestablish functional

autophagy flux along with enhanced mitochondrial autophagy, which, in combination, reduces myocardial I/R injury. Moreover, the restored autophagy provided by Dex was eliminated by 3-MA, and the protective effects of Dex on the I/R heart were partially reversed by 3-MA, as reflected by the dropped heart function.

ROS have been shown to regulate autophagy by modulating AMPK, a key energy sensor that regulates cellular metabolism to maintain energy homeostasis.[28,40] Autophagy is enhanced during the ischemia process through AMPK activation in response to low ATP levels.[39,54,55] Previous studies reported that AMPK deficiency exacerbates myocardial I/R injury, which supports the results of inhibited AMPK expression in the I/R heart.[7,56] In addition, SIRT3 is regulated by AMPK and closely linked to autophagy in the heart.[27,57] A significant decline in the SIRT3 protein levels in the I/R heart, which can be restored by Dex, was observed in the current study.[58] The SIRT family is a group of histone deacetylases whose activities are dependent on and regulated by NAD^+.[59,60] Sergey et al reported that SIRT3 reduces vascular inflammation and oxidative stress, and Duan et al reported that NAD^+ repletion improves ischemia cardiomyocyte outcomes.[61,62] In line with previous studies, the ratio of NAD^+/NADH is decreased in the I/R heart, while Dex raises the ratio of NAD^+/NADH, supporting the benefits of Dex on mitochondrial respiration as NAD^+ reflects the function of mitochondrial redox homeostasis.[63–65] More importantly, the AMPK inhibitor Compound C not only significantly suppressed the expression of AMPK and SIRT3, but also impeded the augmentation of Dex-induced autophagy, thereby attenuating the protective effect of Dex on I/R cardiac function. This finding underscores the critical role of AMPK/SIRT3 activation in facilitating Dex-mediated enhancement of autophagy. Given the intricate alterations in autophagy during I/R, it is imperative to focus on different time points to accurately evaluate the effects of Dex on the myocardium during I/R. Additionally, other autophagy detection methods can be used, such as cardiac tissue sections stained for LC3 and the autophagy probe mt-Keima. Certainly, it is essential to utilize transgenic models to validate the role of Dex-mediated autophagy in alleviating myocardial I/R injury, particularly through the AMPK/SIRT3 pathway.

Conclusion

First, this study suggested that Dex manifests protective effects in cardiac I/R injury both in vivo and in vitro, as shown in Figure 5. Next, we proposed that Dex plays critical roles in antioxidant and anti-inflammatory activities using comprehensive experimental methods when I/R is induced. Mechanistically, Dex promoted autophagy through the

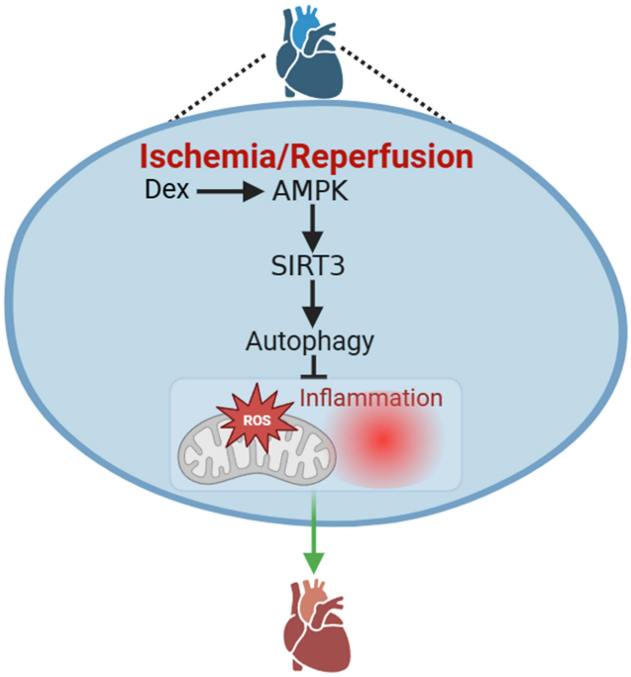

Figure 5 The underlying mechanism involved in the protective effects of DEX against cardiac I/R injury. Created with BioRender.com.

activation of the AMPK/SIRT3 pathway, thus mitigating cardiac I/R injury, which helped expand the prospect of Dex in clinical applications.

Funding

This work is supported by the Science and Technology Plan Project of Sichuan Province, China (2022YFS0439, 2022NSFSC1567, 2023YFS0137), Sichuan Provincial Cadre Health Research Fund (2022-221), and the National Natural Science Foundation of China (82170634).

Disclosure

The authors report no conflicts of interest in this work.

References

1. Xiang M, Lu Y, Xin L, et al. Role of oxidative stress in reperfusion following myocardial ischemia and its treatments. *Oxid Med Cell Longev*. 2021;2021:6614009. doi:10.1155/2021/6614009
2. Ibáñez B, Heusch G, Ovize M, Van de Werf F. Evolving therapies for myocardial ischemia/reperfusion injury. *J Am Coll Cardiol*. 2015;65 (14):1454–1471. doi:10.1016/j.jacc.2015.02.032
3. Cai C, Guo Z, Chang X, et al. Empagliflozin attenuates cardiac microvascular ischemia/reperfusion through activating the AMPKα1/ULK1/ FUNDC1/mitophagy pathway. *Redox Biol*. 2022;52:102288. doi:10.1016/j.redox.2022.102288
4. Wang J, Toan S, Zhou H. New insights into the role of mitochondria in cardiac microvascular ischemia/reperfusion injury. *Angiogenesis*. 2020;23 (3):299–314. doi:10.1007/s10456-020-09720-2
5. Bugger H, Pfeil K. Mitochondrial ROS in myocardial ischemia reperfusion and remodeling. *Biochim Biophys Acta Mol Basis Dis*. 2020;1866 (7):165768. doi:10.1016/j.bbadis.2020.165768
6. Chouchani ET, Pell VR, Gaude E, et al. Ischaemic accumulation of succinate controls reperfusion injury through mitochondrial ROS. *Nature*. 2014;515(7527):431–435. doi:10.1038/nature13909
7. Bou-Teen D, Kaludercic N, Weissman D, et al. Mitochondrial ROS and mitochondria-targeted antioxidants in the aged heart. *Free Radic Biol Med*. 2021;167:109–124. doi:10.1016/j.freeradbiomed.2021.02.043
8. Gao C, Wang R, Li B, et al. TXNIP/Redd1 signalling and excessive autophagy: a novel mechanism of myocardial ischaemia/reperfusion injury in mice. *Cardiovasc Res*. 2020;116(3):645–657. doi:10.1093/cvr/cvz152
9. Weerink M, Struys M, Hannivoort LN, Barends C, Absalom AR, Colin P. Clinical pharmacokinetics and pharmacodynamics of dexmedetomidine. *Clin Pharmacokinet*. 2017;56(8):893–913. doi:10.1007/s40262-017-0507-7
10. Yu W, Lyu J, Jia L, Sheng M, Yu H, Du H. Dexmedetomidine ameliorates hippocampus injury and cognitive dysfunction induced by hepatic ischemia/reperfusion by activating SIRT3-mediated mitophagy and inhibiting activation of the NLRP3 inflammasome in young rats. *Oxid Med Cell Longev*. 2020;2020:7385458. doi:10.1155/2020/7385458
11. Mei B, Li J, Zuo Z. Dexmedetomidine attenuates sepsis-associated inflammation and encephalopathy via central α2A adrenoceptor. *Brain Behav Immun*. 2021;91:296–314. doi:10.1016/j.bbi.2020.10.008
12. Sun YB, Zhao H, Mu DL, et al. Dexmedetomidine inhibits astrocyte pyroptosis and subsequently protects the brain in in vitro and in vivo models of sepsis. *Cell Death Dis*. 2019;10(3):167. doi:10.1038/s41419-019-1416-5
13. Shi J, Yu T, Song K, et al. Dexmedetomidine ameliorates endotoxin-induced acute lung injury in vivo and in vitro by preserving mitochondrial dynamic equilibrium through the HIF-1a/HO-1 signaling pathway. *Redox Biol*. 2021;41:101954. doi:10.1016/j.redox.2021.101954
14. Zhao Y, Feng X, Li B, et al. Dexmedetomidine protects against lipopolysaccharide-induced acute kidney injury by enhancing autophagy through inhibition of the PI3K/AKT/mTOR pathway. *Front Pharmacol*. 2020;11:128. doi:10.3389/fphar.2020.00128
15. Wang Z, Wu J, Hu Z, et al. Dexmedetomidine alleviates lipopolysaccharide-induced acute kidney injury by inhibiting p75NTR-mediated oxidative stress and apoptosis. *Oxid Med Cell Longev*. 2020;2020:5454210. doi:10.1155/2020/5454210
16. Yang YF, Wang H, Song N, et al. Dexmedetomidine attenuates ischemia/reperfusion-induced myocardial inflammation and apoptosis through inhibiting endoplasmic reticulum stress signaling. *J Inflamm Res*. 2021;14:1217–1233. doi:10.2147/JIR.S292263
17. Song J, Du J, Tan X, Wu Z, Yuan J, Cong B. Dexmedetomidine protects the heart against ischemia reperfusion injury via regulation of the bradykinin receptors. *Eur J Pharmacol*. 2021;911:174493. doi:10.1016/j.ejphar.2021.174493
18. Yang FY, Zhang L, Zheng Y, Dong H. Dexmedetomidine attenuates ischemia and reperfusion-induced cardiomyocyte injury through p53 and forkhead box O3a (FOXO3a)/p53-upregulated modulator of apoptosis (PUMA) signaling signaling. *Bioengineered*. 2022;13(1):1377–1387. doi:10.1080/21655979.2021.2017611
19. Levine B, Kroemer G. Biological functions of autophagy genes: a disease perspective. *Cell*. 2019;176(1–2):11–42. doi:10.1016/j.cell.2018.09.048
20. Sciarretta S, Maejima Y, Zablocki D, Sadoshima J. The role of autophagy in the heart. *Annu Rev Physiol*. 2018;80(1):1–26. doi:10.1146/annurev-physiol-021317-121427
21. Shirakabe A, Ikeda Y, Sciarretta S, Zablocki DK, Sadoshima J. Aging and autophagy in the heart. *Circ Res*. 2016;118(10):1563–1576. doi:10.1161/CIRCRESAHA.116.307474
22. Xing Y, Sui Z, Liu Y, et al. Blunting TRPML1 channels protects myocardial ischemia/reperfusion injury by restoring impaired cardiomyocyte autophagy. *Basic Res Cardiol*. 2022;117(1):20. doi:10.1007/s00395-022-00930-x
23. Bravo-San Pedro JM, Kroemer G, Galluzzi L. Autophagy and mitophagy in cardiovascular disease. *Circ Res*. 2017;120(11):1812–1824. doi:10.1161/CIRCRESAHA.117.311082
24. Dong Y, Chen H, Gao J, Liu Y, Li J, Wang J. Molecular machinery and interplay of apoptosis and autophagy in coronary heart disease. *J Mol Cell Cardiol*. 2019;136:27–41. doi:10.1016/j.yjmcc.2019.09.001

25. Del Re DP, Amgalan D, Linkermann A, Liu Q, Kitsis RN. Fundamental mechanisms of regulated cell death and implications for heart disease. *Physiol Rev*. 2019;99(4):1765–1817. doi:10.1152/physrev.00022.2018
26. Wang Z, Sun R, Wang G, et al. SIRT3-mediated deacetylation of PRDX3 alleviates mitochondrial oxidative damage and apoptosis induced by intestinal ischemia/reperfusion injury. *Redox Biol*. 2020;28:101343. doi:10.1016/j.redox.2019.101343
27. Zhai M, Li B, Duan W, et al. Melatonin ameliorates myocardial ischemia reperfusion injury through SIRT3-dependent regulation of oxidative stress and apoptosis. *J Pineal Res*. 2017:63. doi:10.1111/jpi.12419
28. Lin SC, Hardie DG. AMPK: sensing glucose as well as cellular energy status. *Cell Metab*. 2018;27(2):299–313. doi:10.1016/j.cmet.2017.10.009
29. Zhang Y, Wang Y, Xu J, et al. Melatonin attenuates myocardial ischemia-reperfusion injury via improving mitochondrial fusion/mitophagy and activating the AMPK-OPA1 signaling pathways. *J Pineal Res*. 2019;66(2):e12542. doi:10.1111/jpi.12542
30. Chen C, Chen Y, Liu T, Song D, Ma D, Cheng O. Dexmedetomidine can enhance PINK1/Parkin-mediated mitophagy in MPTP-Induced PD mice model by activating AMPK. *Oxid Med Cell Longev*. 2022;2022:7511393. doi:10.1155/2022/7511393
31. Yang T, Feng X, Zhao Y, et al. Dexmedetomidine enhances autophagy via α2-AR/AMPK/mTOR pathway to inhibit the activation of NLRP3 inflammasome and subsequently alleviates lipopolysaccharide-induced acute kidney injury. *Front Pharmacol*. 2020;11:790. doi:10.3389/fphar.2020.00790
32. Wang Y, Mao X, Chen H, et al. Dexmedetomidine alleviates LPS-induced apoptosis and inflammation in macrophages by eliminating damaged mitochondria via PINK1 mediated mitophagy. *Int Immunopharmacol*. 2019;73:471–481. doi:10.1016/j.intimp.2019.05.027
33. Zhu Z, Ling X, Zhou H, Zhang C. Dexmedetomidine at a dose of 1 μM attenuates H9c2 cardiomyocyte injury under 3 h of hypoxia exposure and 3 h of reoxygenation through the inhibition of endoplasmic reticulum stress. *Exp Ther Med*. 2021;21(2):132. doi:10.3892/etm.2020.9564
34. Mittal M, Siddiqui MR, Tran K, Reddy SP, Malik AB. Reactive oxygen species in inflammation and tissue injury. *Antioxid Redox Signal*. 2014;20(7):1126–1167. doi:10.1089/ars.2012.5149
35. Ou W, Liang Y, Qin Y, et al. Hypoxic acclimation improves cardiac redox homeostasis and protects heart against ischemia-reperfusion injury through upregulation of O-GlcNAcylation. *Redox Biol*. 2021;43:101994. doi:10.1016/j.redox.2021.101994
36. Blaser H, Dostert C, Mak TW, Brenner D. TNF and ROS crosstalk in inflammation. *Trends Cell Biol*. 2016;26(4):249–261. doi:10.1016/j.tcb.2015.12.002
37. Zhang X, Wei M, Fan J, et al. Ischemia-induced upregulation of autophagy preludes dysfunctional lysosomal storage and associated synaptic impairments in neurons. *Autophagy*. 2021;17(6):1519–1542. doi:10.1080/15548627.2020.1840796
38. Dikic I, Elazar Z. Mechanism and medical implications of mammalian autophagy. *Nat Rev Mol Cell Biol*. 2018;19(6):349–364. doi:10.1038/s41580-018-0003-4
39. Herzig S, Shaw RJ. AMPK: guardian of metabolism and mitochondrial homeostasis. *Nat Rev Mol Cell Biol*. 2018;19(2):121–135. doi:10.1038/nrm.2017.95
40. Hu Y, Chen H, Zhang L, et al. The AMPK-MFN2 axis regulates MAM dynamics and autophagy induced by energy stresses. *Autophagy*. 2021;17(5):1142–1156. doi:10.1080/15548627.2020.1749490
41. Kane AE, Sinclair DA. Sirtuins and NAD + in the development and treatment of metabolic and cardiovascular diseases. *Circ Res*. 2018;123(7):868–885. doi:10.1161/CIRCRESAHA.118.312498
42. Diao Z, Ji Q, Wu Z, et al. SIRT3 consolidates heterochromatin and counteracts senescence. *Nucleic Acids Res*. 2021;49(8):4203–4219. doi:10.1093/nar/gkab161
43. Wang T, Li Z, Xia S, Xu Z, Chen X, Sun H. Dexmedetomidine promotes cell proliferation and inhibits cell apoptosis by regulating LINC00982 and activating the phosphoinositide-3-kinase (PI3K)/protein kinase B (AKT) signaling in hypoxia/reoxygenation-induced H9c2 cells. *Bioengineered*. 2022;13(4):10159–10167. doi:10.1080/21655979.2022.2060900
44. Eid RA, Bin-Meferij MM, El-Kott AF, et al. Exendin-4 protects against myocardial ischemia-reperfusion injury by upregulation of SIRT1 and SIRT3 and activation of AMPK. *J Cardiovasc Transl Res*. 2021;14(4):619–635. doi:10.1007/s12265-020-09984-5
45. Lu Y, Nanayakkara G, Sun Y, et al. Procaspase-1 patrolled to the nucleus of proatherogenic lipid LPC-activated human aortic endothelial cells induces ROS promoter CYP1B1 and strong inflammation. *Redox Biol*. 2021;47:102142. doi:10.1016/j.redox.2021.102142
46. Li A, Gao M, Liu B, et al. Mitochondrial autophagy: molecular mechanisms and implications for cardiovascular disease. *Cell Death Dis*. 2022;13(5):444. doi:10.1038/s41419-022-04906-6
47. Hamacher-Brady A, Brady NR, Gottlieb RA. Enhancing macroautophagy protects against ischemia/reperfusion injury in cardiac myocytes. *J Biol Chem*. 2006;281(40):29776–29787. doi:10.1074/jbc.M603783200
48. Li Y, Liang P, Jiang B, et al. CARD9 promotes autophagy in cardiomyocytes in myocardial ischemia/reperfusion injury via interacting with Rubicon directly. *Basic Res Cardiol*. 2020;115(3):29. doi:10.1007/s00395-020-0790-6
49. Yu YW, Liu S, Zhou YY, et al. Shexiang baoxin pill attenuates myocardial ischemia/reperfusion injury by activating autophagy via modulating the ceRNA-Map3k8 pathway. *Phytomedicine*. 2022;104:154336. doi:10.1016/j.phymed.2022.154336
50. Xie M, Kong Y, Tan W, et al. Histone deacetylase inhibition blunts ischemia/reperfusion injury by inducing cardiomyocyte autophagy. *Circulation*. 2014;129(10):1139–1151. doi:10.1161/CIRCULATIONAHA.113.002416
51. Qin GW, Lu P, Peng L, Jiang W. Ginsenoside Rb1 inhibits cardiomyocyte autophagy via PI3K/Akt/mTOR signaling pathway and reduces myocardial ischemia/reperfusion injury. *Am J Chin Med*. 2021;49(08):1913–1927. doi:10.1142/S0192415X21500907
52. Rabinovich-Nikitin I, Rasouli M, Reitz CJ, et al. Mitochondrial autophagy and cell survival is regulated by the circadian Clock gene in cardiac myocytes during ischemic stress. *Autophagy*. 2021;17(11):3794–3812. doi:10.1080/15548627.2021.1938913
53. Zeng X, Zhang YD, Ma RY, et al. Activated Drp1 regulates p62-mediated autophagic flux and aggravates inflammation in cerebral ischemia-reperfusion via the ROS-RIP1/RIP3-exosome axis. *Mil Med Res*. 2022;9(1):25. doi:10.1186/s40779-022-00383-2
54. Lee H, Zandkarimi F, Zhang Y, et al. Energy-stress-mediated AMPK activation inhibits ferroptosis. *Nat Cell Biol*. 2020;22(2):225–234. doi:10.1038/s41556-020-0461-8
55. Wen J, Xu B, Sun Y, et al. Paeoniflorin protects against intestinal ischemia/reperfusion by activating LKB1/AMPK and promoting autophagy. *Pharmacol Res*. 2019;146:104308. doi:10.1016/j.phrs.2019.104308
56. Tao L, Gao E, Jiao X, et al. Adiponectin cardioprotection after myocardial ischemia/reperfusion involves the reduction of oxidative/nitrative stress. *Circulation*. 2007;115(11):1408–1416. doi:10.1161/CIRCULATIONAHA.106.666941

57. Xu K, He Y, Moqbel S, Zhou X, Wu L, Bao J. SIRT3 ameliorates osteoarthritis via regulating chondrocyte autophagy and apoptosis through the PI3K/Akt/mTOR pathway. *Int J Biol Macromol*. 2021;175:351–360. doi:10.1016/j.ijbiomac.2021.02.029
58. Yang J, He J, Ismail M, et al. HDAC inhibition induces autophagy and mitochondrial biogenesis to maintain mitochondrial homeostasis during cardiac ischemia/reperfusion injury. *J Mol Cell Cardiol*. 2019;130:36–48. doi:10.1016/j.yjmcc.2019.03.008
59. Wu QJ, Zhang TN, Chen HH, et al. The sirtuin family in health and disease. *Signal Transduct Target Ther*. 2022;7(1):402. doi:10.1038/s41392-022-01257-8
60. Chang HC, Guarente L. SIRT1 and other sirtuins in metabolism. *Trends Endocrinol Metab*. 2014;25(3):138–145. doi:10.1016/j.tem.2013.12.001
61. Dikalova AE, Pandey A, Xiao L, et al. Mitochondrial deacetylase sirt3 reduces vascular dysfunction and hypertension while sirt3 depletion in essential hypertension is linked to vascular inflammation and oxidative stress. *Circ Res*. 2020;126(4):439–452. doi:10.1161/CIRCRESAHA.119.315767
62. Cai W, Xu D, Zeng C, et al. Modulating lysine crotonylation in cardiomyocytes improves myocardial outcomes. *Circ Res*. 2022;131(5):456–472. doi:10.1161/CIRCRESAHA.122.321054
63. Rajman L, Chwalek K, Sinclair DA. Therapeutic potential of NAD-boosting molecules: the in vivo evidence. *Cell Metab*. 2018;27(3):529–547. doi:10.1016/j.cmet.2018.02.011
64. Zapata-Pérez R, Wanders R, van Karnebeek C, Houtkooper RH. NAD + homeostasis in human health and disease. *EMBO Mol Med*. 2021;13(7):e13943. doi:10.15252/emmm.202113943
65. Abdellatif M, Sedej S, Kroemer G. NAD + metabolism in cardiac health, aging, and disease. *Circulation*. 2021;144(22):1795–1817. doi:10.1161/CIRCULATIONAHA.121.056589